

Clemson University

TigerPrints

All Theses

Theses

May 2020

Design and Development of an Unconstrained Spine Test Rig to Study the Kinematics of Spine Motion

Nisha Gulhane

Clemson University, gulhane.nisha@gmail.com

Follow this and additional works at: https://tigerprints.clemson.edu/all_theses

Recommended Citation

Gulhane, Nisha, "Design and Development of an Unconstrained Spine Test Rig to Study the Kinematics of Spine Motion" (2020). *All Theses*. 3261.

https://tigerprints.clemson.edu/all_theses/3261

This Thesis is brought to you for free and open access by the Theses at TigerPrints. It has been accepted for inclusion in All Theses by an authorized administrator of TigerPrints. For more information, please contact kokeefe@clemson.edu.

DESIGN AND DEVELOPMENT OF AN UNCONSTRAINED SPINE TEST RIG TO STUDY THE KINEMATICS OF SPINE MOTION

A Thesis
Presented to
the Graduate School of
Clemson University

In Partial Fulfillment
of the Requirements for the Degree
Master of Science
Bioengineering and Biomedical Engineering

by
Nisha Gulhane
May 2020

Accepted by:
Melinda Harman, Ph.D., Committee Chair
Jeremy Mercuri, Ph.D.
Hai Yao, Ph.D.

Abstract

The spine is one of the most complex structures in the musculoskeletal system. Surgical procedures and implants used to treat spinal disorders include modification or removal of the diseased intervertebral disk, vertebral fusion using various combinations of hardware devices, and total disc replacement using mobile implant devices. The safety and efficacy of these implants need to be evaluated prior to clinical use. Three-dimensional biomechanical testing of the spine is necessary to evaluate the spine function along with the effects of disorders, surgical procedures and implants. General flexibility tests using pure moments can be performed using commercially available testing frames, but they are costly and not available in many research labs. The setup developed in this study can be accommodated by any lab with a bi-axial testing machine. The test rig designed in this study allows for the unconstrained motion of the spine under pure moment loading conditions. Loading can be applied continuously or in a stepwise fashion through positive and negative moments. The motion data was captured using Polaris Vicra, NDI Digital. This data was then analyzed using a custom code written in MATLAB, (Mathworks, Natick, MA). A mechanical analog lumbar spine model was used for kinematic experiments and the study showed promising results for the test rig to be used as an unconstrained spine test rig.

Acknowledgments

I would like to acknowledge my research advisor and mentor, Dr. Melinda Harman, who has been a constant support throughout my journey in this department and has played a vital role in shaping me as a Bioengineer. Thank you so much for giving me an opportunity to work on this research. I also acknowledge the guidance received from my committee members, Dr. Jeremy Mercuri and Dr. Hai Yao. I thank the faculty and staff of the Bioengineering Department for creating a great environment to learn and grow. A special thanks to the staff at Machining and Technical Services at Clemson, who went out of their way to guide me through my research.

I would like to acknowledge the support and encouragement from the ReMED lab members, and all the help I received from them. I would also like to thank the Physics and Astronomy department and the General Engineering department for giving me the opportunity to work as a teaching assistant and a graduate teacher, it has been a great learning experience. I would finally like to thank my family and friends for all the love and support. This journey would not have been possible if not for them.

Table of Contents

| | |
|--|------------|
| Title Page | i |
| Abstract | ii |
| Acknowledgments | iii |
| List of Figures | v |
| Abbreviations | vi |
| 1 Introduction | 1 |
| 2 Design and Methods | 4 |
| 2.1 Design: Test Rig | 4 |
| 2.1.1 Construction | 6 |
| 2.1.2 Specimen preparation | 8 |
| 2.1.3 Characteristics | 12 |
| 2.2 Design: Optical motion capturing | 12 |
| 2.2.1 Scope of the MoCap system | 12 |
| 2.2.2 Tools and attachments | 13 |
| 2.2.3 Characteristics | 15 |
| 2.3 Method | 18 |
| 2.3.1 Parameters | 18 |
| 2.3.2 Testing Technique | 18 |
| 3 Experimental Results and Analysis | 21 |
| 3.1 Test rig: Initial setup | 21 |
| 3.2 Kinematic Results | 23 |
| 3.2.1 Lateral Bending | 24 |
| 3.2.2 Flexion- Extension | 28 |
| 3.2.3 Axial Torsion | 29 |
| 3.3 Discussion | 32 |
| 3.4 Assumptions and limitations of the study | 33 |
| 4 Conclusion and Discussion | 36 |
| References | 37 |

List of Figures

| | | |
|------|--|----|
| 2.1 | Complete Assembly | 5 |
| 2.2 | Assembly Description: Loading Assembly | 7 |
| 2.3 | Assembly Description: Base Assembly | 9 |
| 2.4 | Unconstrained spine test rig mounted on the bi-axial testing machine | 10 |
| 2.5 | Acrylic Box sized appropriately for mounting | 11 |
| 2.6 | Bone cement used for potting | 11 |
| 2.7 | Acrylic tool with reflective markers | 14 |
| 2.8 | Custom made attachment | 14 |
| 2.9 | Tool assembled with the attachment | 14 |
| 2.10 | CT Scan showing fiducial markers (metal balls) | 15 |
| 2.11 | Local coordinate system defined using fiducial markers, (figure on the left is a CAD model generated from CT Scan data) | 16 |
| 2.12 | x-y table stage with vernier scale | 17 |
| 2.13 | Numbered grids on the x-y stage platform | 17 |
| 2.14 | General Load-deflection behavior of a human spine. Arrows indicate loading and unloading directions. (Neutral zone (NZ), Extension zone (EZ), Range of motion (ROM) | 18 |
| 2.15 | Three cycles of lateral bending at a 0.5deg/sec loading rate to achieve a maximum moment of approximately $\pm 6Nm$ | 20 |
| 3.1 | Local Coordinate System: Variability | 22 |
| 3.2 | Representative variation in the origin and axes of the LCS | 23 |
| 3.3 | Load-Displacement Curve for Lateral bending test: displacement measured using the optical motion capture data and Instron load cell | 24 |
| 3.4 | Intersegmental bending ROM's percentage contribution | 25 |
| 3.5 | Stiffness data from literature [12] and this study under $\pm 6Nm$ pure moment | 25 |
| 3.6 | Load-Displacement Curve for L2-L3 during the lateral bending test | 26 |
| 3.7 | Load-Displacement Curve for L3-L4 during the lateral bending test | 26 |
| 3.8 | Load-Displacement Curve for L4-L5 during the lateral bending test | 27 |
| 3.9 | Load-Displacement Curve for Flexion-extension test. Displacement measured using the optical motion capture data and Instron load cell is displayed. Stiffness graph from literature [11] is also shown | 28 |
| 3.10 | Load-Displacement Curve for Axial Torsion test. Displacement measured using the optical motion capture data and Instron load cell is displayed | 29 |
| 3.11 | Approximate intersegmental ROM over the complete cycle | 29 |
| 3.12 | Load-Displacement Curve for L2-L3 during the axial torsion test | 30 |
| 3.13 | Load-Displacement Curve for L3-L4 during the axial torsion test | 30 |
| 3.14 | Load-Displacement Curve for L4-L5 during the axial torsion test | 31 |

Abbreviations

LBP Lower Back Pain

ROM Range of Motion

DOF Degree of Freedom

MoCap Motion Capturing

NZ Neutral Zone

EZ Extension Zone

LCS Local or Anatomical coordinate system

Chapter 1

Introduction

The broad objective of this thesis is to evaluate spine biomechanics using an *in-vitro* biomechanical spine simulator. This objective will be accomplished in two aims:

Aim 1) Design and validate a mechanical testing rig that can be attached to a standard bi-axial testing machine; and

Aim 2) Define and implement a protocol for the optical motion capture for kinematic measurements using a validated biomechanical synthetic lumbar spine analog model.

Successful completion of these aims will produce a standardized *in-vitro* test method for assessing unconstrained spine biomechanics in the spine simulator.

Significance: Spinal disorders such as lower back pain (LBP) caused by intervertebral disc degeneration are major health problems around the globe. In the United States, 70 – 90% people have LBP at some point in their life [1]. According to the survey of the National Center for Health Statistics, in the United States, more than 500,000 back and neck surgeries were performed annually in 2006. The second most cited reason for physician visits in the United States is back pain [2]. From 2005 to 2015, the global burden of LBP and years lived with lower back and neck pain increased by nearly 20% [3]. Pain induced due to these diseases negatively affects daily activities, workforce productivity, and the overall efficiency of an individual. Thus, the need for improving the lives of these individuals has resulted in a rise in demand for better spinal implants.

The spine is one of the most complex structures in the musculoskeletal system and the disorders contributing to LBP affect different regions of the spine. Surgical procedures and implants used to treat spinal disorders include modification or removal of the diseased intervertebral disk,

vertebral fusion using various combinations of hardware devices, and total disc replacement using mobile implant devices. Out of these, spinal fusion had become a common procedure after the '90s showing rapid growth of 220% surgeries till 2001 [4]; however, the health improvements after surgeries are not very satisfactory. Hence, alternative approaches like disc replacements have gained research interests [5].

Challenges: Given that the safety and efficacy of new treatments and implant devices must be demonstrated before clinical use [6], there is a high demand for developing suitable predictive models (e.g. experimental or computational simulations) for better and repeatable evaluations. In many cases, the process by which tests are carried out is difficult to understand and it makes it difficult to compare two separate implants for their quality and test performance results [6]. There are certain standard protocols that help overcome this problem; however, the latest technologies for motion-preserving spinal implants may not have the necessary standard test established by ASTM International or ISO [6]. Along with differences in testing procedures, the specimen variability may also produce misleading results. Biomechanical evaluation of the biological models to test the implants is a common procedure. Although, the anatomy and mechanical properties such as range of motion and stiffness between and porcine spine are shown to be similar [7], there are still challenges regarding the change in mechanical properties with time, the instrumentation on the soft tissue, and variability in height, weight, age, and health of the animal prior to testing. For example, up to a 500% variation was found in normal disc pressures between different cadaveric specimens [8].

The spinal column consists of 24 vertebral bones (7 cervical, 12 thoracic, 5 lumbar) and 23 fibrocartilaginous intervertebral discs. These crucial structures protect the spinal cord while maintaining trunk stability and allowing for complex spinal motions during activities of daily living. Flexion and extension motion occurs in the sagittal plane, bending occurs in the front plane, rotation occurs in the transverse plane. These primary rotational movements along with translational movements (i.e. anteroposterior, latero-lateral, and craniocaudal) define the six degrees of freedom for an individual spinal unit (e.g. two vertebral bones separated by one intervertebral disc). Spine exhibits a coupled motion, that is, the local motions of the individual spinal units combine in a kinematic chain that produces global motions of the entire spinal column. Hence it is complicated to define. Multisegmental spine kinematics to describe coupled motions cannot be directly assessed by calculating centers of rotation, instead, helical axes are to be defined [9]. Optical motion capturing systems are used in conjunction with the loading setup for determining these complicated motions.

To standardize the *in-vitro* biomechanical test protocol, one accepted method is to apply a load control approach in an unconstrained manner. However, the displacement control method has the advantage of applying translation or rotation inputs based on the required motion. It also has the best supporting literature data for most biomechanical situations that can be used in the validation study for this research. The scientific literature for *in-vitro* spine testing is very extensive and involves a variety of biomechanical spine simulators. Generally, all simulators include an actuator, load cell, a system to mount a specimen, and a system to measure intersegmental motion/ pressure according to the test aims [9]. They are unique in the mechanisms used to apply loads and achieve unconstrained motion. While expensive robotic test systems exist (e.g. MTS Bionix), many labs already have existing bi-axial test frames that are suitable when used with a proper test rig and coupled with validated computational algorithms for calculating relative vertebral motions.

Technical Gap: Due to the above challenges, there is a need for a mechanical test rig that is capable of applying known pure moments along multi-segmental spine specimens and is easily coupled with a motion capture system for measuring the kinematics of individual vertebral bones. **Chapter 2** provides the details of the design and methods and a review of the challenges discussed earlier with reference to the test rig characteristics. **Chapter 3** of this thesis provides experimental results of the spine analog and validation of the *in-vitro* biomechanical spine simulator through comparison with existing experimental data from other labs using the spine analog. **Chapter 4** of this thesis provides a discussion of the results and recommendations for future work.

Chapter 2

Design and Methods

To achieve accurate results, in-vivo load conditions must be simulated during laboratory tests. When complex motions are to be studied, spine simulators have been found to be the most common approach. To achieve accurate results, in-vivo load conditions must be simulated during laboratory tests. When complex motions are to be studied, spine simulators have been found to be the most common approach. Pure moment loading to achieve bending simulations have been widely accepted [9].

This chapter is divided into three sections:

1. First section describes the design of the test rig.
2. Second section describes the design of the motion capturing system tools and attachments.

It will also explain the terminologies and the motion capturing protocol.

3. Third section explains the methods used for validating the setup and protocol used for carrying out torsion, bending and flexion-extension tests.

2.1 Design: Test Rig

A biomechanical test rig is designed using SOLIDWORKS and fabricated at a local machine shop. The setup allows for unconstrained spine kinematic tests similar to a published study [10]. It accommodates potted spine specimens, including both synthetic lumbar spine models (Sawbones) and physiological specimens (e.g. oxtail or human cadaver). The rig consists of two sections: the load assembly attached to the bi-axial testing machine's (Instron 8864, Instron Corp, Norwood,

Massachusetts) load cell and the translation assembly that provides five DOFs for unconstrained tests.



Figure 2.1: Complete Assembly

2.1.1 Construction

Loading Assembly: It is attached to the load cell for transmitting torsional forces to the potted blocks or caudal end of the spine. This attachment can be fixed in a vertical as well as a horizontal position.

Base Assembly: It holds the bottom of the distal end of the spine and is fixed to the test frame. This fixture has multiple orientations based on the test being carried out. The x-y table provides translational DOF while the swivel axis that holds the pocket allows for one rotational DOF. There are two more DOF that can be controlled based on the requirement. The spline shaft and linear bearing arrangement allowed vertical translation. The bearing that holds the pocket mounting shaft provides for another DOF which can be locked using a shaft collar if needed.

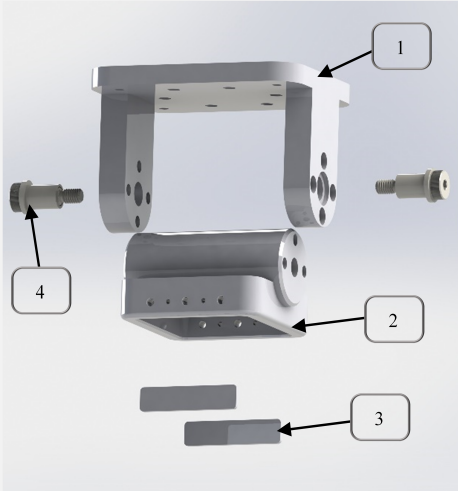
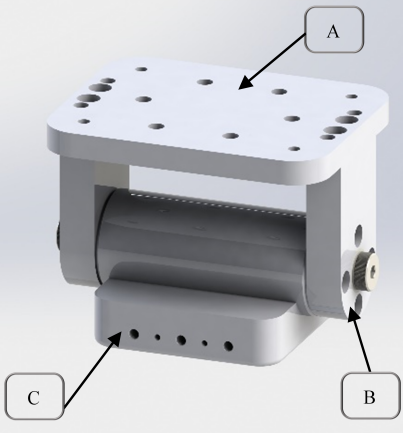
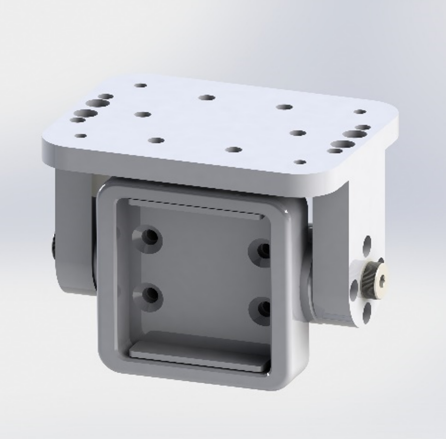
| Subassembly | Components and Configuration | Characteristics |
|-------------------------|---|---|
| Loading Assembly |  | <ol style="list-style-type: none"> 1. Fixed to the load cell at surface 'A' and transfers torsion to the whole setup 2. Pocket acts as a specimen holder and it can be fixed in horizontal or vertical orientation w.r.t '1' 3. Clamping plates hold specimen in place 4. Flanged sleeve bearing and shoulder screw arrangement |
| |  | <p>Vertical configuration</p> <p>Torsion applied by load cell will result in axial rotation of the specimen.</p> <p>Screws at 'B' lock orientation of the loading assembly while grub screws at 'C' lock specimen in place.</p> |
| |  | <p>Horizontal configuration</p> <p>Torsion applied by load cell will result in lateral bending and flexion-extension motion of the specimen.</p> <p>Unlock loading assembly's rotation once specimen is mounted.</p> |

Figure 2.2: Assembly Description: Loading Assembly

Angle measuring plate The angle measuring plate helps define the start point for every experiment. If there is any permanent deformation in the specimen, it can be identified by the change in orientation. Under higher loads, change in height may also be reported.

2.1.2 Specimen preparation

Pacific Research Laboratories have developed synthetic mechanical analog spine models [11]. The synthetic spine models consist of polyurethane foam vertebral bodies connected with intervertebral discs, ligaments and facet capsules consisting of various polyester/urethane polymers. The specimen is held at each end that sits in a pocket and is secured using grub screws. The size of the pockets was determined based on the Sawbones biomechanical model.

In case, any other specimen is to be mounted, a box made out of acrylic sheets of the same dimensions was also made to secure the specimen using bone cement. Figure 2.6 shows an ox-tail mounted using the custom-made box potted with bone cement.

Orientation of the spine is to be taken care of when mounting it manually. The PRL analog lumbar spine is manufactured in such a way that the axis passing through L3-L4 is kept vertical [12].

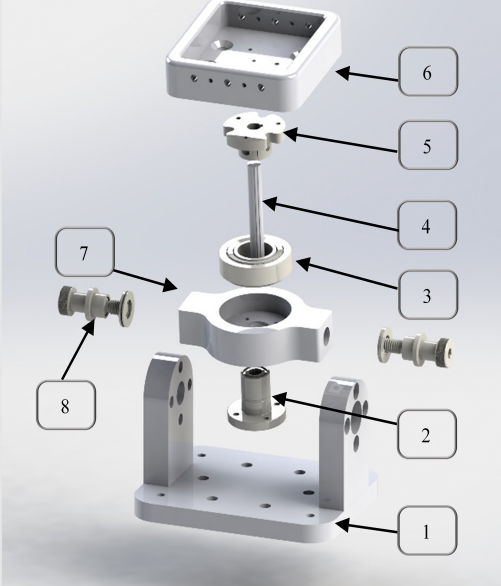
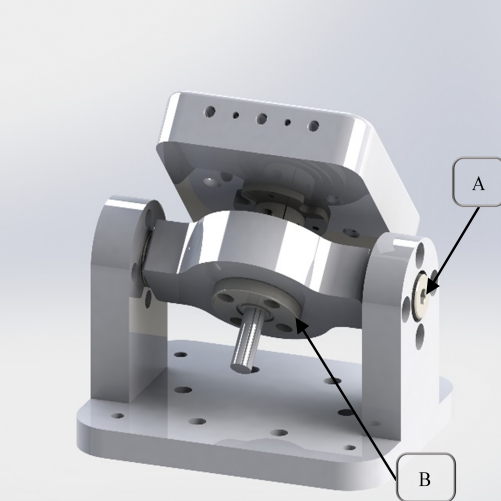
| Subassembly | Components and Configuration | Characteristics |
|---|---|--|
| <p style="text-align: center;">Base Assembly</p> |  | <ol style="list-style-type: none"> 1. Fixed to the X-Y table for free translational motion (2DOF) 2. Linear bearing holds spline shaft '4', passes through roller bearing '3' and has mounting holes on the flange 3. Roller bearing (1DOF) 4. Spline shaft for vertical linear motion (1DOF) 5. Flanged shaft collar forms an interface between '6' and '4' 6. Pocket acts as a specimen holder 7. Bearing holder with swivel arrangement through point 'A' 8. Flanged sleeve bearing and shoulder screw arrangement (1DOF) |
| |  | <p>Configurations:</p> <p>The base assembly provides 5DOF to the testing environment</p> <ul style="list-style-type: none"> • Torsion test: Use the mounting holes and screws to lock rotation for '2'. • Bending test: Lower load cell and move base assembly to accommodate horizontal position of the specimen. • A clamp is provided (not shown in figure) to lock the spline shaft translation if needed |

Figure 2.3: Assembly Description: Base Assembly

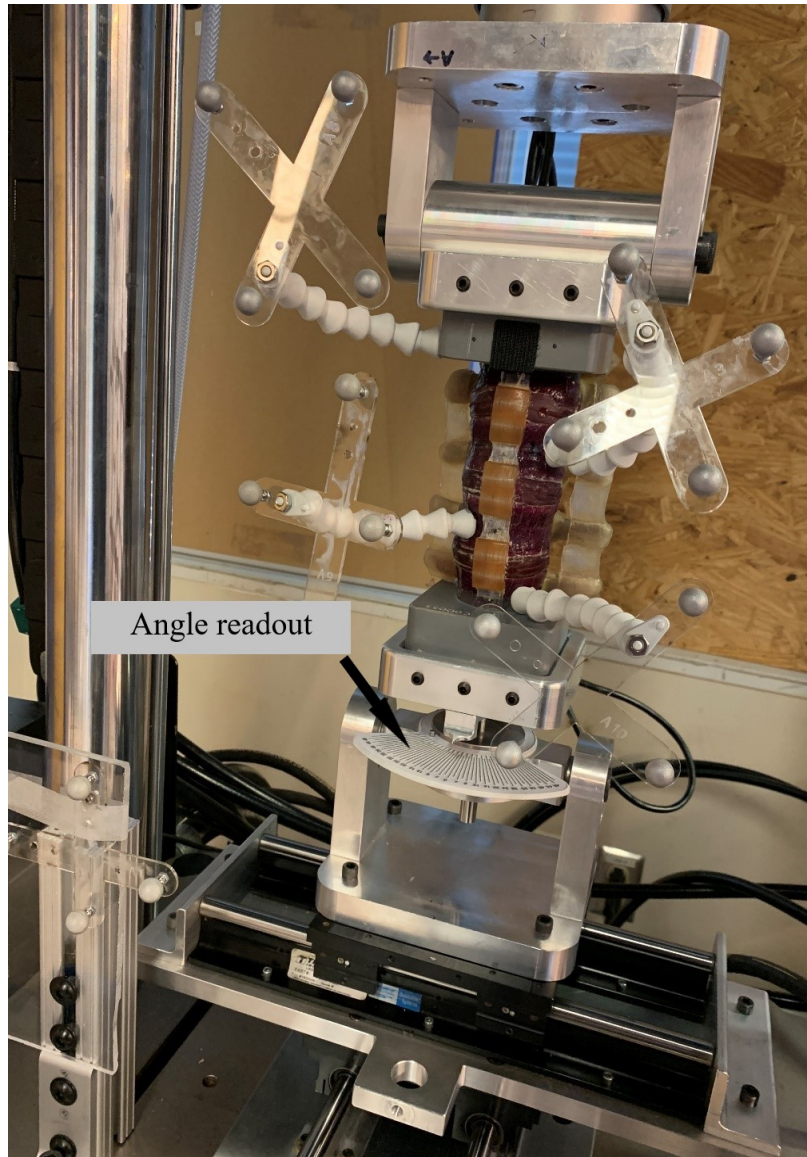


Figure 2.4: Unconstrained spine test rig mounted on the bi-axial testing machine



Figure 2.5: Acrylic Box sized appropriately for mounting

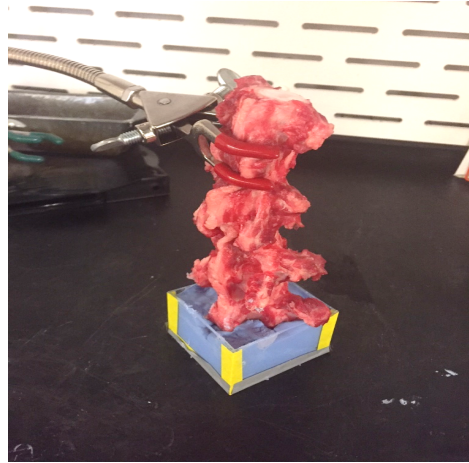


Figure 2.6: Bone cement used for potting

2.1.3 Characteristics

The following characteristics are described based on the recommended testing criteria for spinal implants [13].

- a. The specimen is free to move in all six degrees of freedom.
- b. The simulator is capable of applying pure moments along all three axes.
- c. Loading can be applied continuously or in a step-wise fashion
- d. Positive and negative moments can be applied continuously.

The load cell used is a $\pm 25kN(\pm 5620lbf)$, $\pm 100Nm(\pm 880in - lb)$ Biaxial Dynacell manufactured by INSTRON. It is designed for use with dynamic testing systems and has the ability to measure forces as low as $1/250^{th}$ of the force capacity to an accuracy of 0.5% of reading. Torques applied in this study are very low compared to the capacity of this load cell.

2.2 Design: Optical motion capturing

A three-dimensional motion analysis protocol has been developed that allows measurement of the relative movement of the vertebral bodies. The relative motion between two rigid bodies can be defined in multiple ways, one of which was developed by Grood and Suntay[14]. This method eliminates the sequence dependency of Euler Angles. In this model the initial orientation i, j, k more to its final orientation i', j', k' without having to follow a specific rotation sequence.

2.2.1 Scope of the MoCap system

This test method covers material and method for kinetic testing of a lumbar spine. It describes the following steps:

- a. Define anatomical coordinate system (LCS)
- b. Obtain motion data for each vertebra using NDI Polaris Vicra
- c. Calculate relative motion using Matlab

System Polaris Vicra: An optical tracking system (Polaris Vicra- Northern Digital Incorporation, Ontario, Canada) is used. It can measure the position in 3D space of the instrument-specific markers with a $0.25mm$ RMS accuracy. The system uses passive or active markers that define unique tools for defining position in its frame of reference. The passive tools consist of markers with a retro-reflective coating that reflects infrared (IR) light back to its source. The position sensors of

the Vicra system collect IR light reflected from passive markers and calculate the transformations of the tools.

NDI 6D architect software is used to create tool definition files that include the geometry of the tools. Other information such as the marker information, face normals, and parameters needed for tool recognition are also stored in this file.

2.2.2 Tools and attachments

For kinematic measurements, passive tools were fixed rigidly on each vertebral body. There is an open-source database for the tools used by Polaris which is used to manufacture tools used in this study [15]. Tools are made using laser-cut acrylic sheets and non-medical reflective markers obtained from NDI. They were attached to the vertebral body using screws, loc-line joints and a modified loc-line connector as seen in figure 2.7, 2.8 and 2.9.

A handheld digital probe registered the position of the fiducial markers on the vertebral landmarks that defined the local coordinate system (LCS) for each of them. A passive tool fixed on the Instron bed was assigned to be the global coordinate system. Calculation of rigid body kinematics can be done using transformation matrices describing the position of a rigid body in a global or local frame of reference from one instant to the next. A custom MATLAB (MathWorks, Natick, MA) code calculated a relationship between the rigidly attached passive tools and the LCS. The motion detected through these tools was then transformed into the spine motion based on the Grood Suntay coordinate system [14]. The Instron load cell and the optical tracking system operated at $20Hz$ and synced using a manual motion trigger.

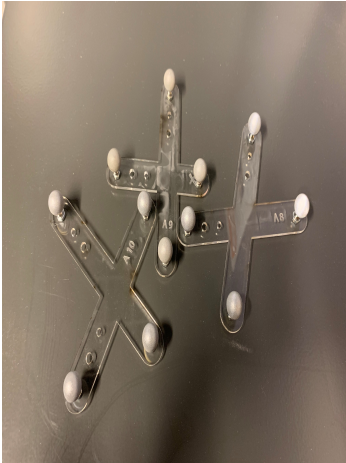


Figure 2.7: Acrylic tool with reflective markers

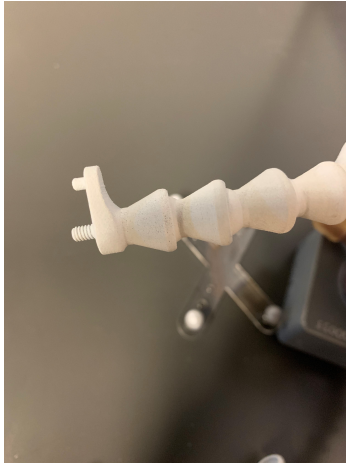


Figure 2.8: Custom made attachment

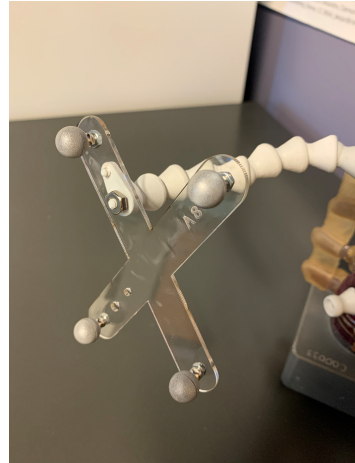


Figure 2.9: Tool assembled with the attachment

Local/ Anatomical coordinate system (LCS) The local coordinate systems for each vertebra are defined based on the bony landmarks. As the Sawbones model does not have clear landmarks, some approximations were made. Metal balls were used as landmarks to define the local coordinate system as seen in the CT Scan image 2.10. These were registered as two most lateral points (L-1, L-3) and the most anterior point (L-2). The origin of the LCS (point O) is defined as the midpoint of the line connecting the most lateral points which also defines the x axis. The vector along O-L-2 is then calculated. z axis is defined as the cross product of the x axis and the vector along O-L-2. The y axis is defined as the cross product of the unit vectors in the x and z direction.

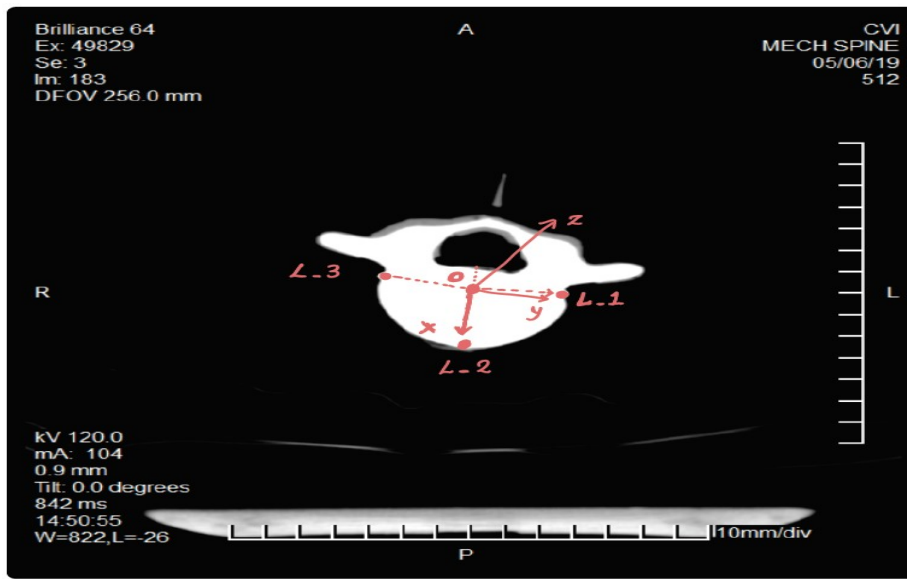


Figure 2.10: CT Scan showing fiducial markers (metal balls)

2.2.3 Characteristics

The motion measurement system's characteristics based on the recommended testing criteria for spinal implants [13] a. The motion capturing system is capable of measuring three-dimensional relative motion between two vertebrae of interest. b. The local coordinate system used in this study needs further modification for the accurate description of intervertebral translational motion with a common axis between two vertebral bodies and located at the vertebral endplates.

The tool definition files used in this study have been validated for inter tool compatibility, pivot calibration and target registration [15]. The pivot tool was defined using the NDI Track

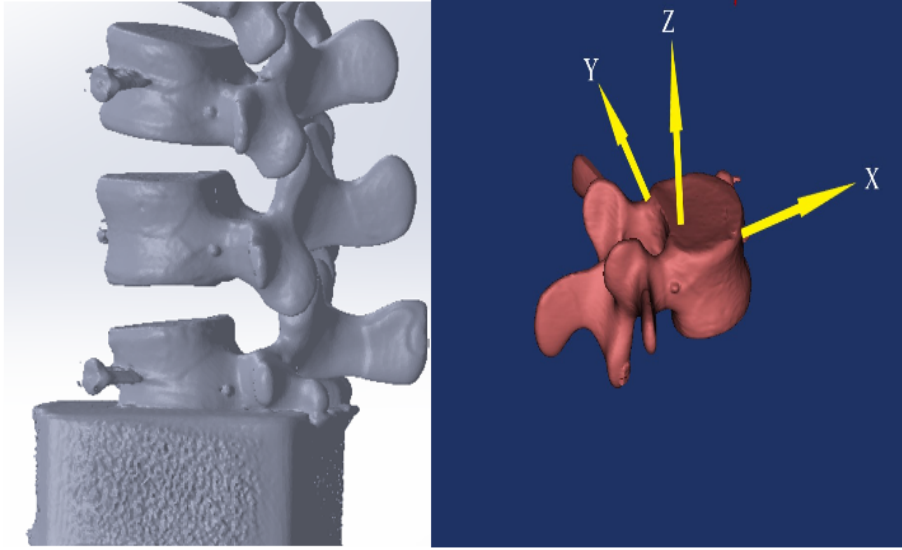


Figure 2.11: Local coordinate system defined using fiducial markers, (figure on the left is a CAD model generated from CT Scan data)

software. The maximum RMS error found during the pivot calibration for 10 trials was $0.36mm$.

One of the tools (Apple-10 [15]) was consistently used for registering fiducial marker positions, hence it was tested for its accuracy. A manual x-y stage with vernier caliper arrangement was used to test the accuracy of the motion capturing system's tool and pivot measurements 2.12. The manual scale has a least count of $0.1mm$. A tool was placed on this table and the table was moved through a virtual grid of 36 points ($5 \times 5cm \pm 2$) within the field of measurement of the Vicra tracker. The expected linear distance between these grid points was 1cm, the standard deviation calculated was $0.42mm$ with a mean of $10.07mm$. A pivot tool was also calibrated by measuring positions of the corners for each grid on the platform as seen in figure 2.13. The linear distance between each grid point was 2cm. The calculated linear distance for each of these grid lines resulted in a mean $20.04mm$ mean and $0.58mm$ standard deviation.

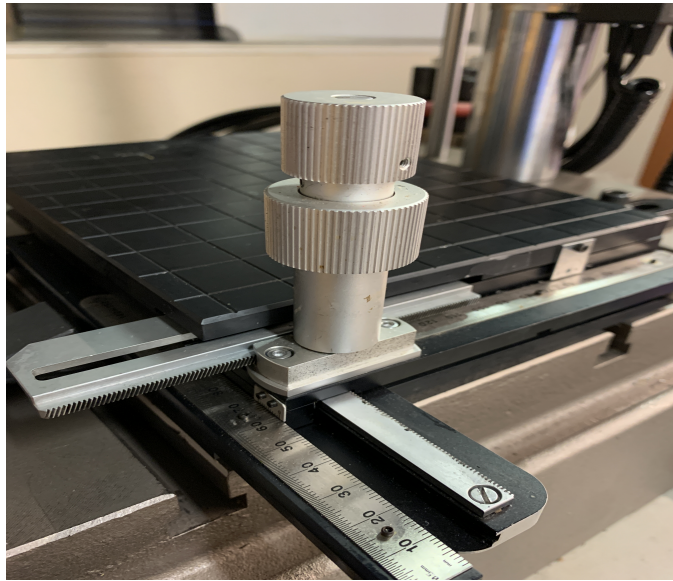


Figure 2.12: x-y table stage with vernier scale

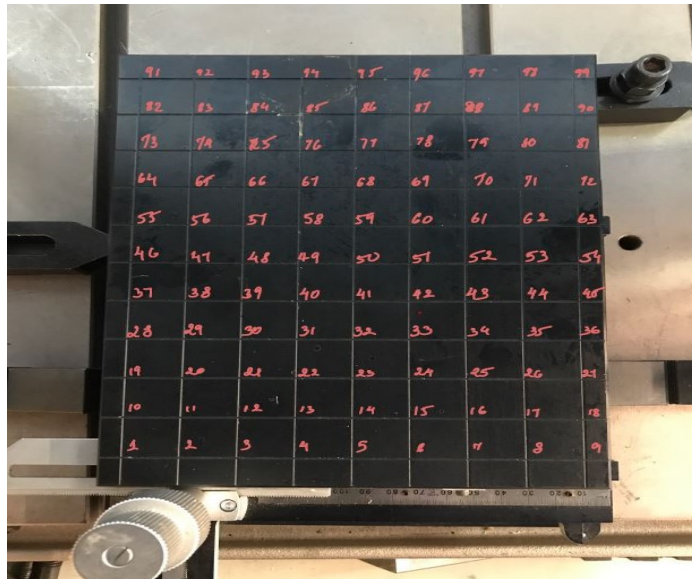


Figure 2.13: Numbered grids on the x-y stage platform

2.3 Method

2.3.1 Parameters

The human spine displays a non-linear behaviour between load and deflection under torsion and bending motions. This behavior is divided into two zones, **neutral and extension/ elastic zone**. In the neutral zone, large deflection occurs without applying appreciable loads, which describes the laxity of the specimen, whereas higher loads are required to induce motions in the extension zone. **ROM** refers to the motion of the segment under physiological loading conditions and is measured in degrees. Many *in-vitro* tests tend to use a **hybrid loading protocol** in which pure moments are applied to identify a global ROM in two different specimens, for example, before and after inserting an implant. **Stiffness** relates to the spine's resistance to deform under loads or moments. Stiffness can be determined from the load-displacement curve as shown in the 2.14.

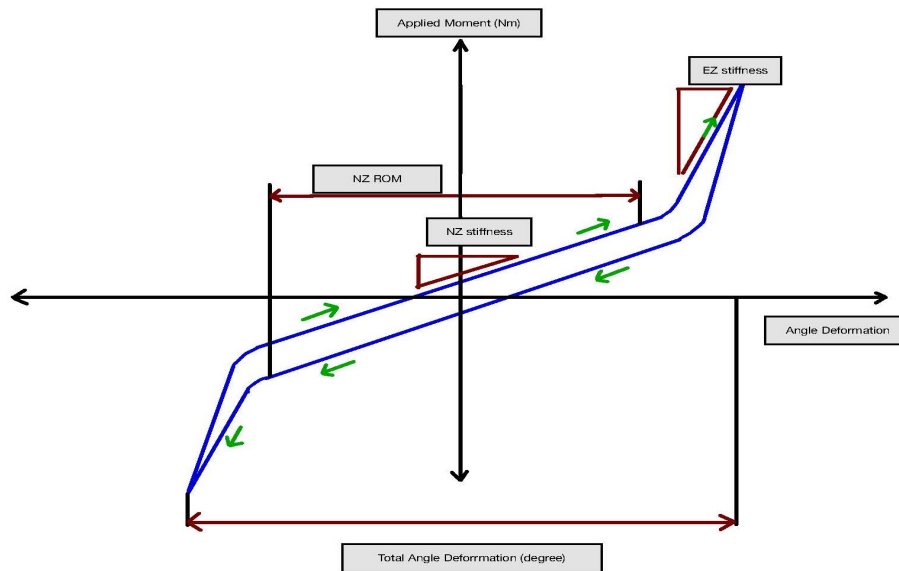


Figure 2.14: General Load-deflection behavior of a human spine. Arrows indicate loading and unloading directions. (Neutral zone (NZ), Extension zone (EZ), Range of motion (ROM))

2.3.2 Testing Technique

It is not possible to quantify the in-vivo loads accurately that include gravity, external loads and the action of the trunk muscles [9]. There is a lot of data available for in-vivo pressure data using

sensors inserted in the discs, which cannot be directly related to the force experienced as it may not be evenly distributed. Thus, the key loading modes simulated in an *in-vitro* test are compression related to the body weight and the counteracting muscle forces and bending required to maintain stability as well as bending in the three principal anatomic planes.

Physiological loading is not achieved when applying pure moments. A follower load concept has been introduced to overcome this issue. A compressive follower load with a path approximating the tangent to the curve of the lumbar spine can be introduced to achieve better representation of in-vivo loads on the spine [16]. Preloading resembles real-life situations and it changes ROM as well as the load-bearing capacity of the spine significantly. The latest MTS Bionix Spine Kinematic System[17] also suggests using an optional load follower in conjunction with the unconstrained tests to accommodate body mass influences. It can be achieved by passing a cable through eyelets attached to the vertebral body and applying dead weights or constant loads using a load cell through this cable.

When complex motions are to be studied, spine simulators have been found to be the most common approach. Pure moment loading conditions to achieve bending simulations have been widely accepted [9]. Typical values for the applied moments are $7.5Nm$ for lumbar specimens, $5Nm$ for thoracic specimens, and $2.5Nm$ for specimens harvested from the lower cervical spine[13]. Achieving these conditions is complex. It is not possible to simulate complex patterns of motion using a single component of force, or to maintain control over test conditions with near-zero stiffness as the displacement can change with no change in the load- input[13]. The load experienced at various levels should be constant and it should not constrain the motion[9]. There can be two possible approaches: **load control** and **position control**. To standardize the *in-vitro* biomechanical test protocol, one accepted method is to apply a load control approach in an unconstrained manner. However, the displacement control method has the advantage of applying translation or rotation inputs based on the required motion. It also has the best supporting literature data for most biomechanical situations that can be used in the validation study for this research. We have used the displacement control approach in this study.

In this study, one analog lumbar spine(L2 through L5) was tested. Tests were carried out at room temperature. No preloads were applied. The analog model was tested in the following modes of loading

1. Right to left lateral bending
2. Flexion extension bending
3. Axial Torsion

Care was taken to mount the spine in the pocket tightly. Once the mounting was complete, the loading assembly swivel axis was set free. The displacement of the load cell was iteratively adjusted to obtaining a net moment of $6Nm$ for lateral bending and $10Nm$ for flexion-extension bending. The rate of loading was kept constant at $0.5degrees/sec$. This low rate was utilized to facilitate a more accurate comparison with literature data for quasi-static studies[18]. Each test was carried out for three cycles and data from the third cycle was used for further analysis. Figure 2.15 shows that all three cycles have similar trends. However, this trend may change if the specimen is subjected to multiple cycles as shown by a study carried out by Wang *et al* [19]. According to this study, the ROM for a FSU obtained from Sawbones showed a logarithmic growth with cycle number. The data collected during the tests was used to plot moment vs deflection graphs that were used for ROM and stiffness calculations. Net angular motions from load cell should be very close to the global ROM, hence load cell moment vs. displacement graphs were also used for comparison. They are not equivalent due to the coupled motions in other directions.

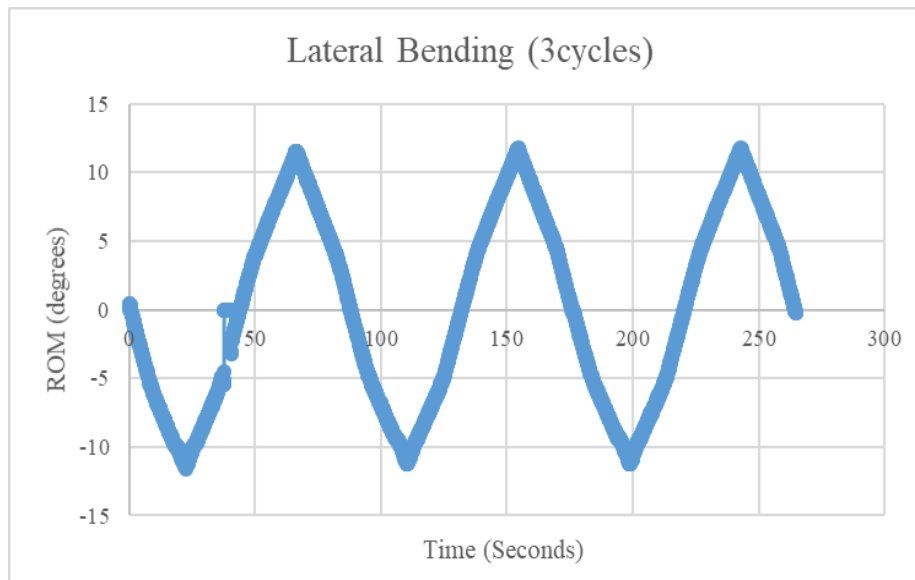


Figure 2.15: Three cycles of lateral bending at a $0.5deg/sec$ loading rate to achieve a maximum moment of approximately $\pm 6Nm$

Chapter 3

Experimental Results and Analysis

This chapter includes the raw results for the kinematic experiments and their analysis. The key variables of interest are the neutral zone and extension zone ROM and stiffness. Before discussing the biomechanical parameters, the test-rig was tested for its characteristics with respect to axis alignment and repeatability of the initial test conditions.

3.1 Test rig: Initial setup

The variables sources of possible errors were axis alignment, permanent deformation in free state, friction, self weight of the assembly, and so on. Out of these, variability in the axis alignment of the loading plane and variability in the LCS calculations were quantified for understanding the system errors.

Axis alignment: The axis misalignment can be caused mainly due to the grub screws and clamp plates holding the spine mounted block in place. The specimen was assembled 10 times and the variation between the center of the mounting block with respect to the Instron axis was measured. The position of the central axis of the spine mount was measured iteratively using a pivot tool calibrated to the optical tracking system. Multiple points were marked on the spine mount, their locations were registered in each iteration. The maximum variation in the expected and measured distances between the axis and surface points were $\pm 0.635mm$ which means that the axis can be positioned anywhere around the expected axis within a $0.635mm$ radius. The position variability was measured only in one plane, assuming that there will not be any variation across the

z-axis. This variation can easily be reduced in two ways:

1. When tightening the clamp plates using grub screws, do not screw only from one direction. Partially tightening the clamps from both sides greatly reduces this error.

2. Another provision such as locator pins is a suggested modification for better accuracy.

The **local coordinate system** for the load cell and L2 was measured 10 times in the same position. The variability between each trial was assessed. Iterative measurements were carried out using a probe tool. The landmarks defining the LCS for the load cell and L2 were measured. The maximum variability in the results is shown in figure 3.1. As the Instron has easy to locate landmarks, LCS variability was lower compared to the L2 LCS. This variation is caused due to the difficulty in locating the fiducial markers on the vertebral body. An average of multiple data points would be an ideal way to reduce errors induced in this case. Another way to reduce errors would be to use a 3D CAD model obtained from the CT Scan data to define the landmarks that are not easy to locate. Also, repeating the measurements before every test would help avoid error accumulation.

| Component | Origin(mm) | X(degrees) | Y(degrees) | Z(degrees) |
|------------------|-------------------|-------------------|-------------------|-------------------|
| Instron head | 0.38 | 1.92 | 1.02 | 1.67 |
| L2 | 0.87 | 1.56 | 2.34 | 2.56 |

Figure 3.1: Local Coordinate System: Variability

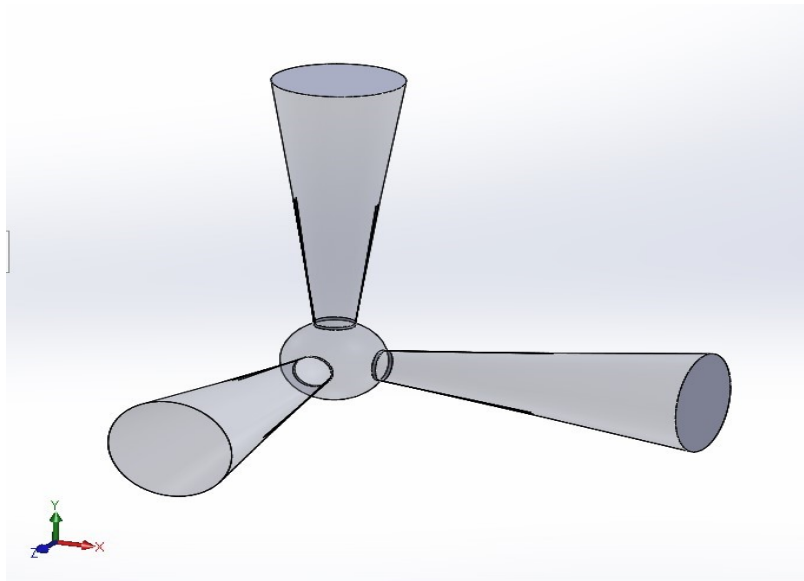


Figure 3.2: Representative variation in the origin and axes of the LCS

3.2 Kinematic Results

This section contains raw kinematic results like stiffness and ROM with comparative literature data. The following tests were carried out

1. Right to Left lateral bending- Bending(right) EZ stiffness, Bending(left) EZ stiffness, ROM
2. Flexion Extension test- Flexion EZ stiffness, Extension EZ stiffness, ROM
3. Axial Torsion- Stiffness, ROM

The graphs displayed in this section include moment data from the load cell, angular global ROM from the load cell (representative of the expected global ROM) and calculated ROM from the data collected using the MoCap system. The load cell ROM shown in graphs is just for reference purpose and does not have direct relation with the global ROM during the tests as the specimen undergoes coupled motions.

3.2.1 Lateral Bending

The mechanical analog spine (L2-L5) exhibited a maximum of 11.73degrees to -11.21degrees of lateral bending under $\pm 6\text{Nm}$ pure moment loading. Total intersegmental motion between L2-L3, L3-L4, L4-L5, and L2-L5 was 2.55degrees , 9.01degrees , 11.38degrees and 22.94degrees respectively. The calculated global ROM and the expected ROM from the Instron load cell data were in close relation with each other as seen in figure 3.3. The range of motion as seen from the stiffness graphs was approximately 8degrees . The EZ stiffness during right and left lateral bending was found to be 0.8124Nm/deg , and 0.998Nm/deg . Figure 3.4 and 3.5 provides complete results for the mechanical analog spine (L2-L5).

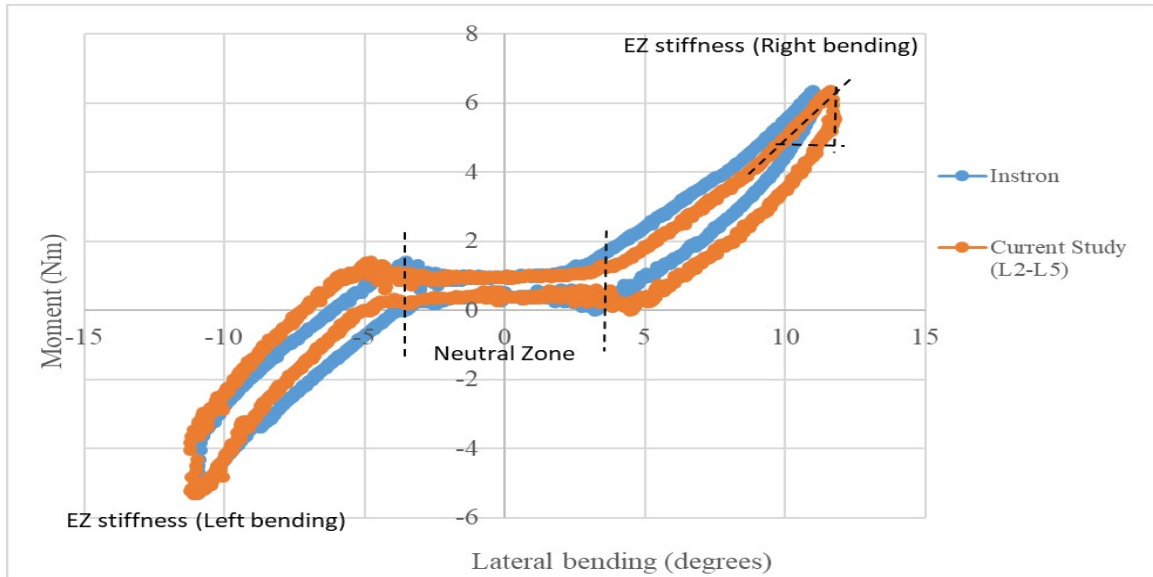


Figure 3.3: Load-Displacement Curve for Lateral bending test: displacement measured using the optical motion capture data and Instron load cell

| Motion | L2-L5 | L2-L3 | L3-L4 | L4-L5 |
|---------------------|-------|--------|--------|--------|
| Right lateral (deg) | 11.73 | 1.72 | 4.41 | 5.48 |
| Left lateral (deg) | 11.21 | 0.83 | 4.60 | 5.90 |
| Total (6Nm) (deg) | 22.94 | 2.55 | 9.01 | 11.38 |
| Contribution (%) | | 11.11% | 39.27% | 49.60% |
| NZ ROM (deg) | ≈8.00 | | | |

Figure 3.4: Intersegmental bending ROM's percentage contribution

| Stiffness | Literature | Current Study |
|----------------------------|------------|---------------|
| EZ Right lateral (N-m/deg) | 1.25±0.3 | 0.8124 |
| EZ Left lateral (N-m/deg) | 1.31±0.27 | 0.998 |
| NZ lateral (N-m/deg) | 0.25±1.3 | NA |

Figure 3.5: Stiffness data from literature [12] and this study under $\pm 6Nm$ pure moment

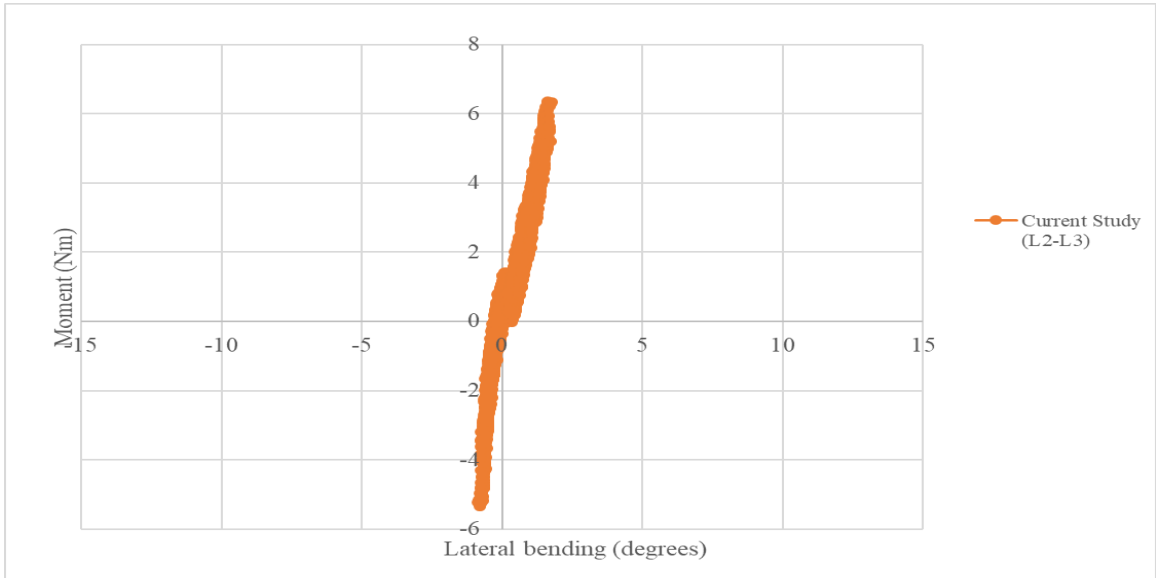


Figure 3.6: Load-Displacement Curve for L2-L3 during the lateral bending test

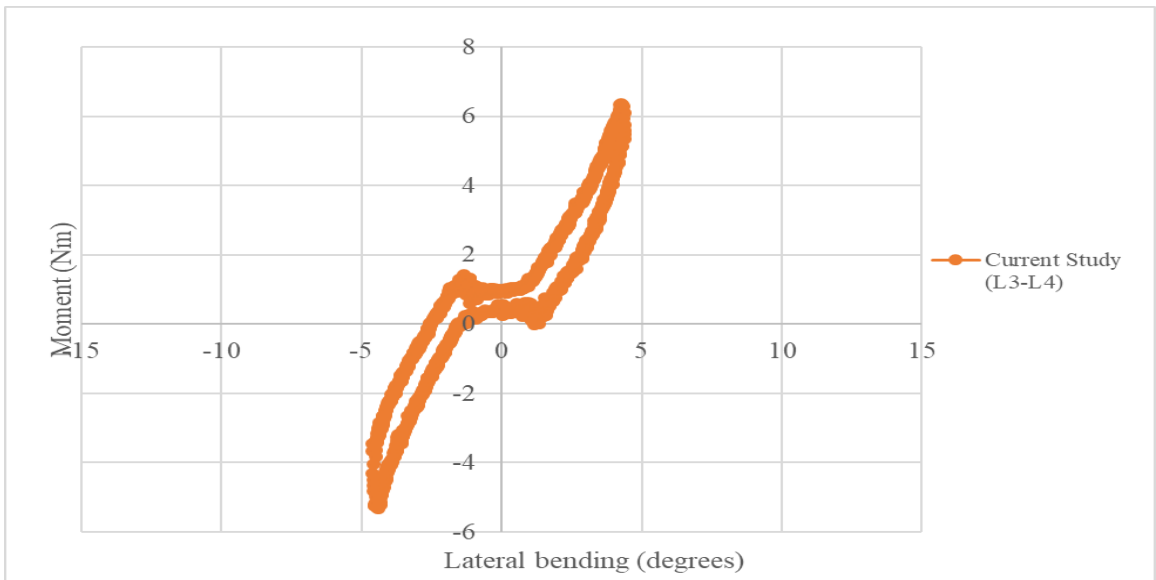


Figure 3.7: Load-Displacement Curve for L3-L4 during the lateral bending test

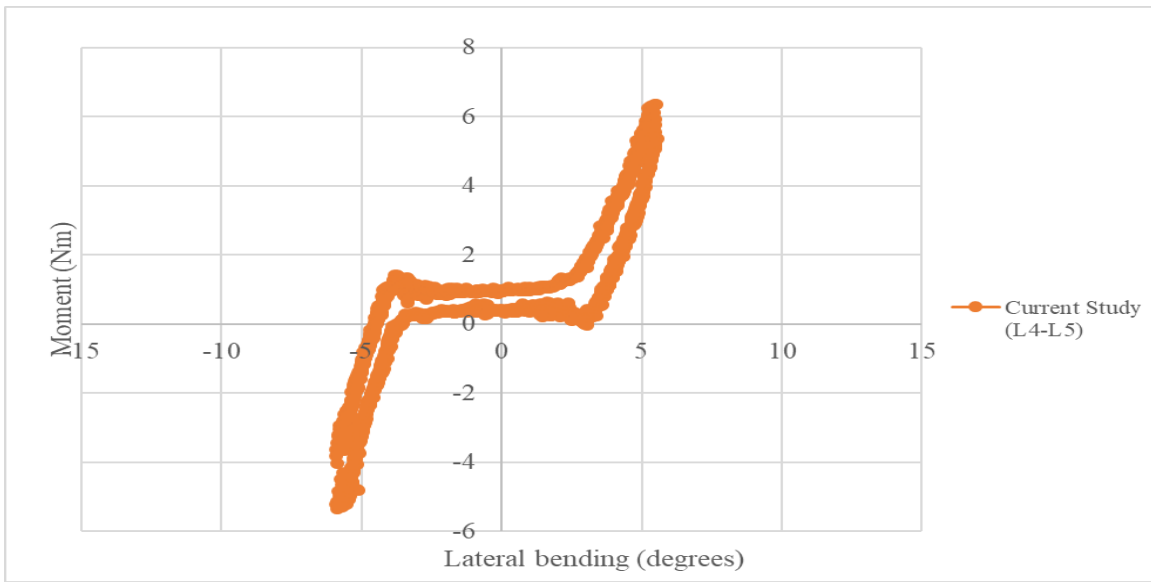


Figure 3.8: Load-Displacement Curve for L4-L5 during the lateral bending test

3.2.2 Flexion- Extension

The flexion-extension tests were carried out such that a maximum of $10Nm$ moments were achieved during the displacement control tests. Stiffness of $0.835N - m/deg$ and $1.680N - /deg$ was observed under flexion and extension respectively. Total ROM calculated was $18.2degrees$.

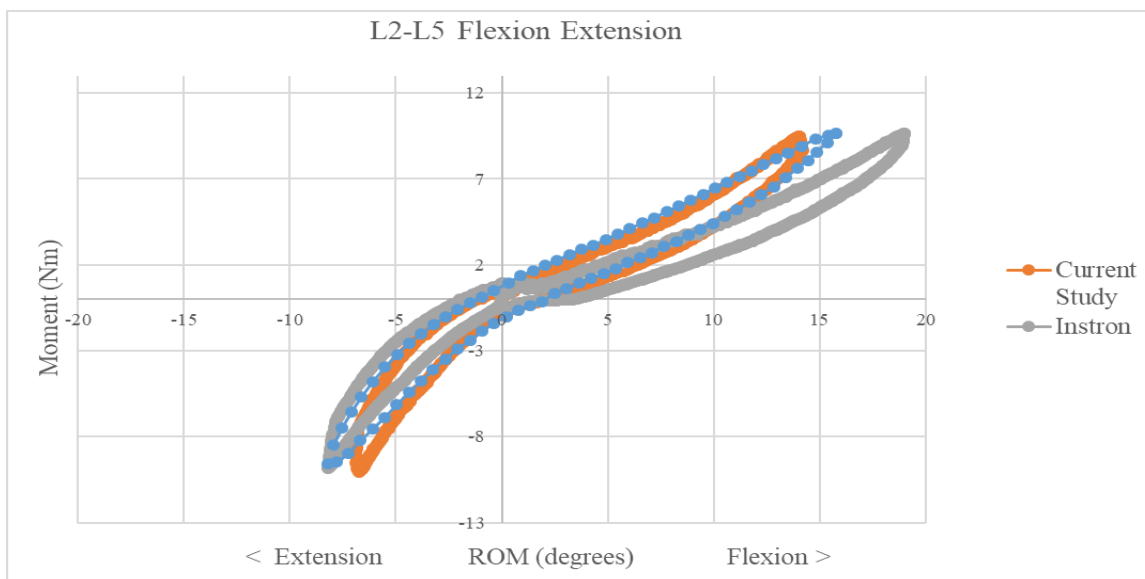


Figure 3.9: Load-Displacement Curve for Flexion-extension test. Displacement measured using the optical motion capture data and Instron load cell is displayed. Stiffness graph from literature [11] is also shown

During the test, some jerky motions were observed. There were two possible reasons for this, firstly the friction of all the sliding components and secondly the imperfect fitting of the spine block in the loading assembly pocket. This was reflected in the results, as can be seen in the graph, the calculated global ROM is less than the load cell's displacement. This error was persistent in multiple tests, hence intersegmental ROMs are not presented in this study. However, the results stiffness graphs shows close relations to the existing literature which makes this method promising.

3.2.3 Axial Torsion

Multiple torsion tests were carried between $6Nm$ to $7.5Nm$ range. The raw data presented below is from one of the tests where $+7.5Nm$ and $-6Nm$ limits were applied to observe the difference on both sides of the load-displacement curves. There is negligible motion seen between L3-L4. Visual inspection also showed that most of the motion was at the caudal end. The stiffness in the extension zones lied between $3.142N - m/deg$ to $3.448Nm/deg$ while the global ROM was $4.41degrees$.

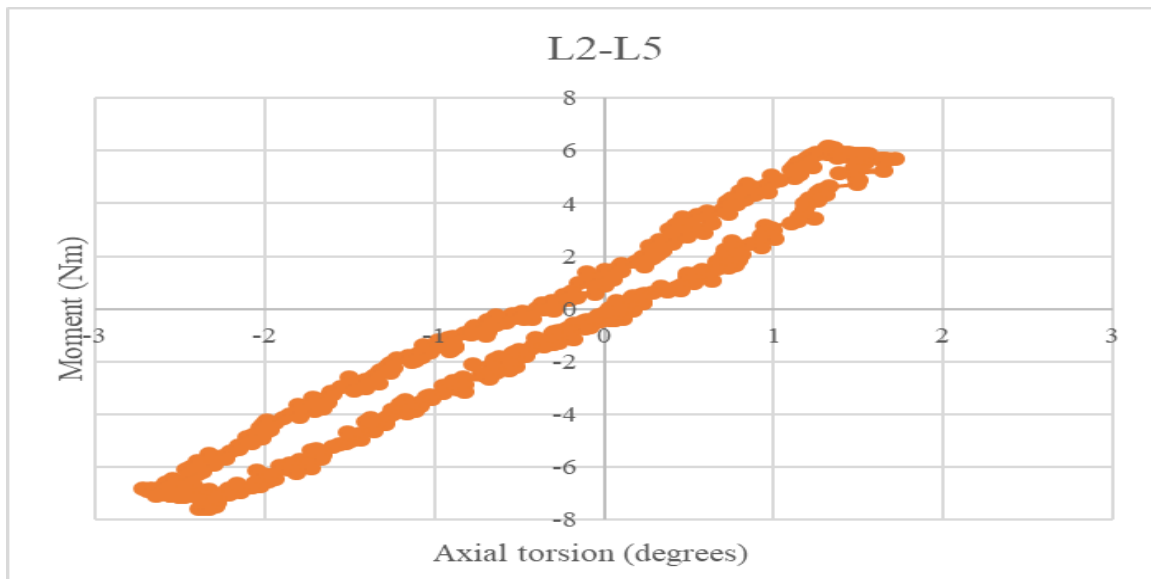


Figure 3.10: Load-Displacement Curve for Axial Torsion test. Displacement measured using the optical motion capture data and Instron load cell is displayed

| Motion | L2-L5 | L2-L3 | L3-L4 | L4-L5 |
|------------------------------------|-------|-------|-------------|-------|
| Total Torsion- $+6Nm-7.5 Nm$ (deg) | 4.41 | 2.89 | ≈ 0 | 1.51 |

Figure 3.11: Approximate intersegmental ROM over the complete cycle

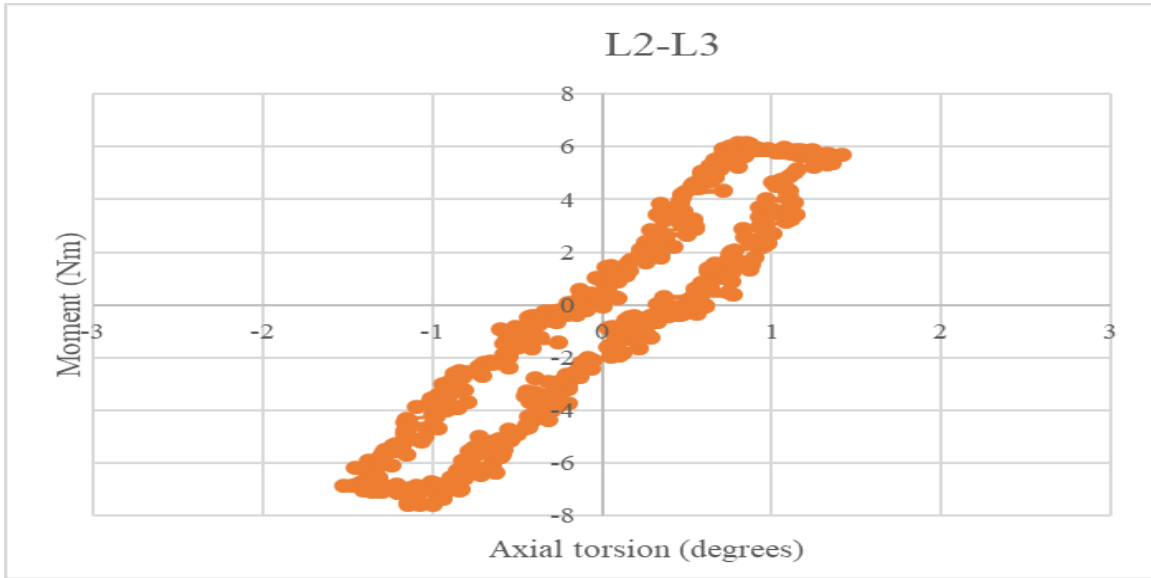


Figure 3.12: Load-Displacement Curve for L2-L3 during the axial torsion test

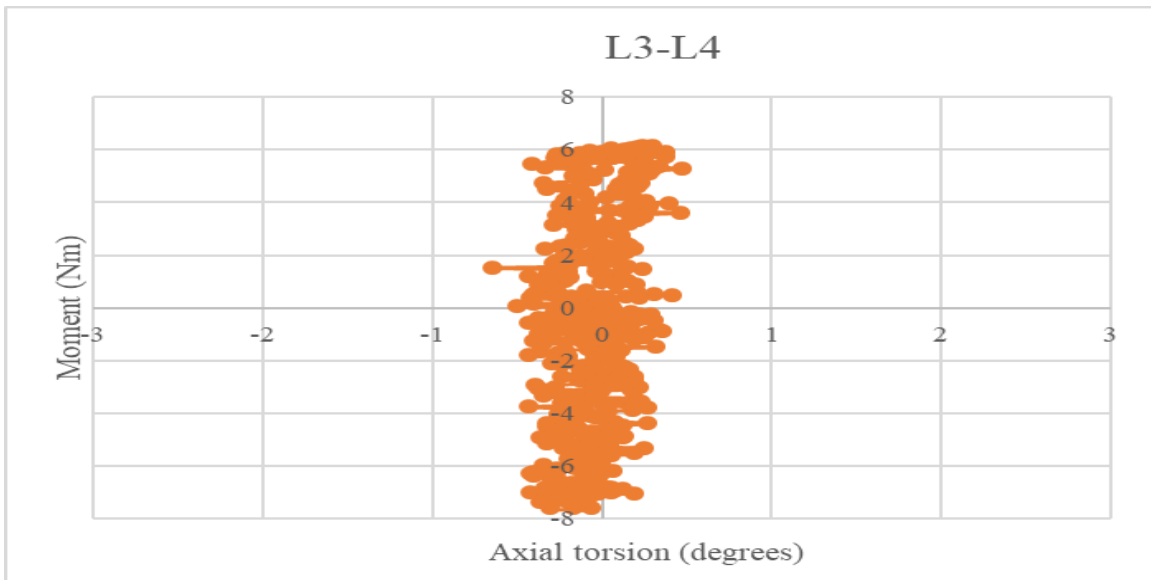


Figure 3.13: Load-Displacement Curve for L3-L4 during the axial torsion test

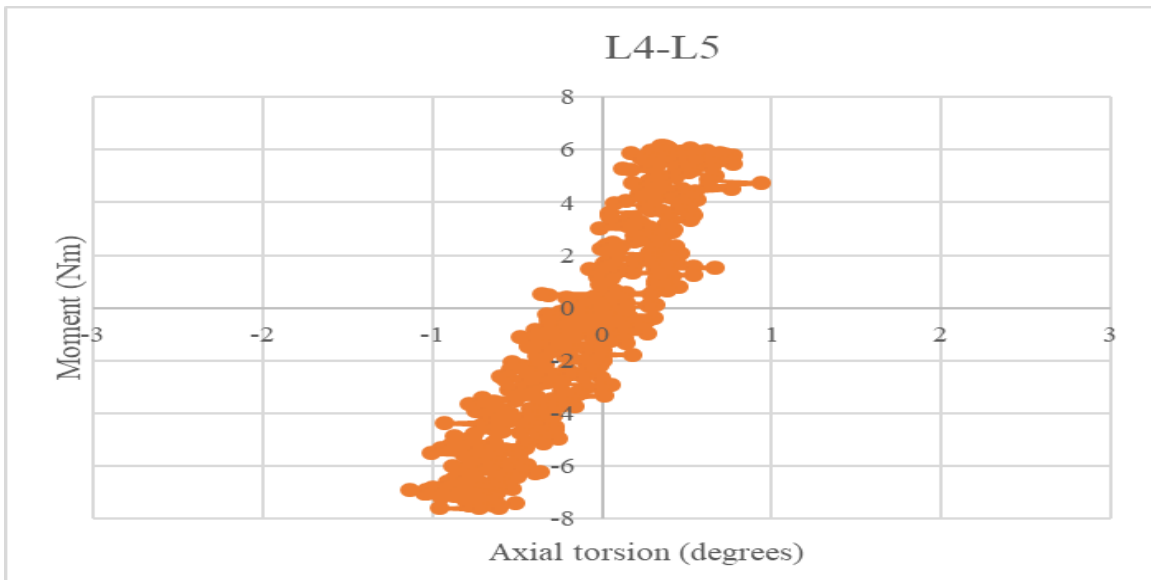


Figure 3.14: Load-Displacement Curve for L4-L5 during the axial torsion test

3.3 Discussion

The broad objective of this thesis was to evaluate spine biomechanical spine simulator. This objective was accomplished by developing an *in-vitro* test method for assessing unconstrained spine biomechanics in the spine test rig. Standard biomechanical tests like flexion-extension, lateral bending and torsion were performed on the analog lumbar spine model using this test-rig.

This thesis benefited from use of a synthetic analog lumbar spine model previously validated against human cadaver spine, as reported in literature. In general, the spine model behaved similar to previous studies, with comparable stiffness values for bending and flexion-extension, while the ROM was different mainly due to the preloading conditions. However direct comparisons with the literature were challenging because of differences in the segment length and test conditions and use of different generation analog models. The literature data available for L2-L5 flexion-extension motion and the preload and test conditions are not clearly identifiable in literature [11]. Lateral bending and stiffness data for T12-L5 spines provided a reference to compare the load-displacement trends in this study. The current study measure higher ROM for the same applied moments due to lack of compressive preloads along the spine axis. Instead, the mass of the base assembly added to a tensile preload in the horizontal position and a tensile preload in the vertical position.

Lateral Bending: Literature data provided in the lateral bending results' tables were from a lateral bending test carried out using a mechanical analog lumbar spine (T12-L5)[12]. There was a very high percentage of NZ variation seen in these tests. The NZ stiffness in this study represents a very low value of $\approx 0N - m/deg$. The EZ right and left bending stiffness values are closer to the lower bounds of the T12-L5 segment. The sum of the intersegmental ROMs was almost equivalent to the global ROM.

Flexion Extension: This data was compared to similar tests carried out by Campbell, J; *et al* [11]. This study had employed an axial load of $2000N$ on a similar analog lumbar spine model (L2-L5) [20]. The corresponding stiffness curve shows a similarity between the two data sets.

Axial Torsion: In literature, the ROM for a single L3-L4 unit is much higher than observed here. The ROM for L3-L4 in this study seem to be rather small because it was part of a full lumbar spine and it acted in-situ, it allows the adjacent segments to rotate and seems like it is floating during the test. Similar observations were made in another study that used analog lumbar spine model (T12 through S1) for biomechanical tests [2]. A FSU (L2-L5) tested under $100N$ preload

for axial torsion had an extension stiffness of $11.25Nm/degree$ [18]. In this study the stiffness was almost one-third of this value which was an expected result.

3.4 Assumptions and limitations of the study

The study focused on achieving an unconstrained test. The concept of the test rig was designed and manufactured to evaluate its functionality. As the design was not completely optimized for mass and functionality, there were some assumptions and limitations associated with this study.

The resulting global mobility of the segments is dependent on the length of the specimen [9]. Limited data is available for the analog lumbar model used in this study. As a sample size of one synthetic lumbar model was used, no statistical analysis was performed on any of the results. Once the design is optimized, the same setup can be used for calculating coupled motions.

One of the errors already discussed earlier may arise from the variability in the anatomical probe points. Three markers are sufficient to define an anatomical/local coordinate system and placed on identifiable landmarks. Firstly, the tools are not rigidly fixed between different tests due to the changing configurations of the specimen, hence the relation between the LCS and tool needs to be defined each time. Secondly, the points were not updated for every other cycle, instead a static shot of the tools acted as a starting point for each subsequent test in that group. In a study by Morton *et al.* [21], the effect of varying the anatomic probe points in the knee was investigated. As per their study, ROM is susceptible to the LCS variability. The rotations in the lumbar spine are small hence variations in anatomic probing may have a large effect on the final ROMs between multiple tests. To reduce marker registration related errors, define the LCS before every test. Take multiple readings for the same data set, and use the average to calculate the ROM. This may help in repeatable data set.

The influence of machine design, mainly friction, may affect the kinematic results. The effect of friction in sliders induces a linearly increasing moment [22] which is compounded in case of multisegmental specimens. The linear bearing components need to be tested for their efficiency, and the manufacturing process needs to be of better quality. The jerky motion during the flexion-extension tests could have been a result of this friction force. Another factor to consider is the hanging mass of the components. For validating the setup, peak off-axis shear loads must be measured. Visual inspection also showed that there were some jerky motions at the starting position, this must have

been due to friction or the specimen not being perfectly held by the clamps provided. Positioning slots or guides and more tightening fixtures can reduce the play occurring during the tests.

When mounting the specimen in the horizontal position, the load cell was lowered to match the base mount height. Only the stroke position of the load cell is shown in the Instron Console software, the global position is not registered. Hence, it was difficult to maintain consistency between tests on different days. In this study, a level indicator was used for better approximation, however, a provision to check the horizontal levels can be included in the future.

The transition from lateral bending to flexion-extension bending needs us to remove the specimen and re-assemble it. A design approach similar to the base assembly can be considered to overcome this step. The transition from torsion (vertical) testing position to the horizontal testing position does not need re-assembling if the length of the specimen is shorter than the analog lumbar spine model. To accommodate different lengths of specimens, the base assembly can be re-designed to provide variable heights.

Cadaver specimens or specimens from another species need additional preparation methods such as freezing, thawing before use and maintaining the temperature and moisture content during the tests. Mounting the spine such that the axis remains vertical will require additional steps. Identifying the landmarks and placing the fiducial markers will be crucial. Using CT-Scan data to identify these landmarks along with being able to measure each one of them with a probe tool for each test may not be convenient. Using CT-Scan data to approximate fiducial marker location can be very useful in these conditions. Another solution could be to use a reference device (3D block) rigidly fixed to each vertebra that protrudes outwards and is easy for target registration; the LCS can be then defined using the transformation obtained from landmarks identified on the CT Scan and the reference's body coordinates defined such that they can be measured using the probe tool during tests [23]. Having a fixed tool attached to each vertebra can also serve the same purpose [24]. But the variety of orientations in this study will obstruct the MoCap view angle in that case.

The LCS defined for the specimen were rough approximations of the expected anatomical landmarks, as the analog spine did not have similar structural features. Re-defining these anatomical landmarks using the CT-Scan data would highly improve the results. If the spine construct is flexible such as a human cervical spine, testing it under the conditions used in this study may not give useful results. Applying a follower load will become necessary in this case. Longer specimens cannot be tested for two reasons: first is the space constraint which can vary depending on the

testing machine used and second is the possibility of errors due to self-weight in the horizontal position (lateral bending and flexion-extension tests). This setup needs to be validated for different lengths of multisegmental spinal constructs.

Chapter 4

Conclusion and Discussion

Overall, the experiments carried out using the spine test rig provided convincing evidence that it will be a reliable model to test and analyze spine biomechanics. While the NZ stiffness is too low in all modes of testing, the specimen stiffness showed close relation with the literature data. Factors such as preloads, follower load and orientation of the spine can affect the measured specimen performance which added to the differences in this study and literature data. A full statistical study changing different parameters needs to be carried out to understand the underlying sources of errors that would help optimize the design further and also validate its repeatability.

Robotic methods applied to *in-vitro* tests offer more comprehensive information, however, simple test rigs like the one presented in this study can also prove to be a useful tool in preliminary evaluations of spine specimens. The fact that it can be coupled with a readily-available bi-axial testing machine would make it easy to standardize tests for a more comparative database.

Experimental testing has some limitations such as difficulty in measuring non-surface stresses and strains, changing experiments or repeating experiments to test different conditions, costs excessive time and labor, failure tests can only be performed once. Subject-specific modeling is another advantage of numerical models. This protocol can also be used to develop standard validation steps for FE models.

Bibliography

1. Brandolini, N., Cristofolini, L. & Viceconti, M. Experimental methods for the biomechanical investigation of the human spine: a review. *Journal of Mechanics in Medicine and Biology* **14**, 1430002 (2014).
2. LaPierre, L. J. *Control of the mechanical properties of the synthetic anterior longitudinal ligament and its effect on the mechanical analogue lumbar spine model* PhD thesis (University of Kansas, 2009).
3. Hurwitz, E. L., Randhawa, K., Yu, H., Côté, P. & Haldeman, S. The Global Spine Care Initiative: a summary of the global burden of low back and neck pain studies. *European Spine Journal* **27**, 796–801 (2018).
4. Deyo, R. A., Gray, D. T., Kreuter, W., Mirza, S. & Martin, B. I. United States trends in lumbar fusion surgery for degenerative conditions. *Spine* **30**, 1441–1445 (2005).
5. Lee, C. K. & Goel, V. K. Artificial disc prosthesis: design concepts and criteria. *The Spine Journal* **4**, S209–S218 (2004).
6. Graham, J. & Estes, B. T. What standards can (and can't) tell us about a spinal device. *International Journal of Spine Surgery* **3**, 178–183 (2009).
7. Wilke, H.-J., Geppert, J. & Kienle, A. Biomechanical in vitro evaluation of the complete porcine spine in comparison with data of the human spine. *European Spine Journal* **20**, 1859–1868 (2011).
8. Cunningham, B. W., Kotani, Y., McNulty, P. S., Cappuccino, A. & McAfee, P. C. The effect of spinal destabilization and instrumentation on lumbar intradiscal pressure: an in vitro biomechanical analysis. *Spine* **22**, 2655–2663 (1997).
9. Galbusera, F. & Wilke, H.-J. *Biomechanics of the Spine: Basic Concepts, Spinal Disorders and Treatments* (Academic Press, 2018).
10. Inceoğlu, S., Chen, J., Cale, H., Harboldt, B. & Cheng, W. K. Unconstrained testing of spine with bi-axial universal testing machine. *Journal of the mechanical behavior of biomedical materials* **50**, 223–227 (2015).
11. Campbell, J., Imsdahl, S. & Ching, R. Evaluation of a synthetic L2-L5 spine model for biomechanical testing. *Canadian Society for Biomechanics/Société Canadienne de Biomécanique (CSB/SCB)* (2012).
12. Dayal, A. & Friis, E. Validation of a synthetic mechanically and anatomically analog lumbar spine model (Masters thesis) (2006).
13. Wilke, H.-J., Wenger, K. & Claes, L. Testing criteria for spinal implants: recommendations for the standardization of in vitro stability testing of spinal implants. *European spine journal* **7**, 148–154 (1998).
14. Grood, E. S. & Suntay, W. J. A joint coordinate system for the clinical description of three-dimensional motions: application to the knee. *Journal of biomechanical engineering* **105**, 136–144 (1983).

15. Brown, A. J., Uneri, A., De Silva, T. S., Manbachi, A. & Siewerdsen, J. H. Design and validation of an open-source library of dynamic reference frames for research and education in optical tracking. *Journal of Medical Imaging* **5**, 021215 (2018).
16. Patwardhan, A. G., Havey, R. M., Meade, K. P., Lee, B. & Dunlap, B. A follower load increases the load-carrying capacity of the lumbar spine in compression. *Spine* **24**, 1003–1009 (1999).
17. MTS Systems Corporation. *Bionix Spine Kinematic System* [Online; accessed Apr 19, 2019]. 2013. https://www.mts.com/cs/groups/public/documents/library/dev_004724.pdf.
18. Domann, J. P. *Development and Validation of an Analogue Lumbar Spine Model and its Integral Components* PhD thesis (University of Kansas, 2011).
19. Wang, T., Ball, J. R., Pelletier, M. H. & Walsh, W. R. Biomechanical evaluation of a biomimetic spinal construct. *Journal of experimental orthopaedics* **1**, 3 (2014).
20. DiAngelo, D., Hoyer, D. & Chung, C. Biomechanical evaluation of a full-length (T12-S) synthetic lumbar spine model. *MOJ App Bio Biomech* **3**, 70–75 (2019).
21. Morton, N. A., Maletsky, L. P., Pal, S. & Laz, P. J. Effect of variability in anatomical landmark location on knee kinematic description. *Journal of Orthopaedic Research* **25**, 1221–1230 (2007).
22. Gédet, P., Thistlethwaite, P. A. & Ferguson, S. J. Minimizing errors during in vitro testing of multisegmental spine specimens: considerations for component selection and kinematic measurement. *Journal of biomechanics* **40**, 1881–1885 (2007).
23. Fischer, K. J., Manson, T., Pfaeffle, H. J., Tomaino, M. & Woo, S.-Y. A method for measuring joint kinematics designed for accurate registration of kinematic data to models constructed from CT data. *Journal of biomechanics* **34**, 377–383 (2001).
24. Holt, C. A., Evans, S. L., Dillon, D. & Ahuja, S. Three-dimensional measurement of intervertebral kinematics in vitro using optical motion analysis. *Proceedings of the Institution of Mechanical Engineers, Part H: Journal of Engineering in Medicine* **219**, 393–399 (2005).